

LBP-Structure Optimization With Symmetry and Uniformity Regularizations for Scene Classification

Jianfeng Ren, *Member, IEEE*, Xudong Jiang, *Senior Member, IEEE*, and Junsong Yuan, *Senior Member, IEEE*

Abstract—Local binary pattern (LBP) and its variants have been widely used in many visual recognition tasks. Most existing approaches utilize predefined LBP structures to extract LBP features. Recently, data-driven LBP structures have shown promising results. However, due to the limited number of training samples, data-driven structures may overfit the training samples, hence could not generalize well on the novel testing samples. To address this problem, we propose two structural regularization constraints for LBP-structure optimization: symmetry constraint and uniformity constraint. These two constraints are inspired by predefined LBP structures, which convey the human prior knowledge on designing LBP structures. The LBP-structure optimization is casted as a binary quadratic programming problem and solved efficiently via the branch-and-bound algorithm. The evaluation on two scene-classification datasets demonstrates the superior performance of the proposed approach compared with both predefined LBP structures and unconstrained data-driven LBP structures.

Index Terms—Local binary pattern (LBP)-structure optimization, scene classification, structural regularization, symmetry constraint, uniformity constraint.

I. INTRODUCTION

LOCAL binary pattern (LBP) and its variants have a wide range of applications, e.g., texture classification [1]–[3], dynamic texture recognition [4]–[6], scene recognition [7]–[10], facial analysis [11]–[19], human detection [20]–[22], and many others [23]–[30]. LBP is popular because of its simplicity, ability to capture image micro-structures, and robustness to illumination variations.

Traditionally, a handcrafted LBP structure was often utilized to extract LBP features [7], [9], [11], [28], [31]–[35]. The most popular LBP structure consists of eight nearest neighbors [7], [9] or P neighbors in a circle [11], [28], [31]. Other geometries, such as line and disk, were explored in local quantized pattern (LQP) [35]. Handcrafted LBP structures are designed based on the human prior knowledge on images, and they may work well across different applications. However, such handcrafted LBP structures may not optimally capture the intrinsic image characteristics of the target application.

Manuscript received September 25, 2016; revised November 10, 2016; accepted November 11, 2016. Date of publication November 23, 2016; date of current version December 20, 2016. This work was supported by the Singapore Future Systems and Technology Directorate (FSTD) under Project reference: MINDEF-NTU-DIRP/2014/01. The associate editor coordinating the review of this manuscript and approving it for publication was Dr. Sebastien Marcel.

The authors are with the School of Electrical & Electronics Engineering, Nanyang Technological University, Singapore 639798 (e-mail: jfren@ntu.edu.sg; exdjiang@ntu.edu.sg; jsyuan@ntu.edu.sg).

Color versions of one or more of the figures in this letter are available online at <http://ieeexplore.ieee.org>.

Digital Object Identifier 10.1109/LSP.2016.2632167

Recently, researchers aim to derive the optimal LBP structures in a data-driven manner. In [14], Maturana *et al.* utilized a heuristic hill-climbing technique to select the suitable LBP structure. Lei *et al.* learnt discriminant image filters and optimal neighborhood sampling strategy in a data-driven way [18]. More recently, Ren *et al.* optimized the LBP structures based on the maximum-joint-mutual-information (MJMI) criterion using binary quadratic programming via the branch-and-bound algorithm [10]. The data-driven LBP structures could well capture the image characteristics of the target application, but they may have the risk of overfitting due to the limited number of training samples.

To address these problems, we propose a new way to incorporate the human knowledge into LBP-structure optimization. We first cast the structure optimization as a point-selection problem based on the maximal-joint-mutual-information criterion [10]. We then extract two design rules from handcrafted LBP structures, i.e., symmetry rule and uniformity rule. Most handcrafted LBP structures are symmetric about the horizontal axis, the vertical axis, and the center pixel. They are also uniformly distributed in different directions at different scales, not closely clustered. This work converts these two design rules into structural regularization constraints for the LBP-structure optimization problem, in the form that could be solved efficiently using binary quadratic programming via the branch-and-bound algorithm. As a result, the final proposed LBP-structure optimization problem with structural constraints could be solved using binary quadratic programming.

The proposed approach is evaluated on two scene-classification datasets: the 21-land-use dataset [36] and the eight-event dataset [37]. It demonstrates superior performance compared with predefined LBP structures, unconstrained data-driven LBP structures, and other state-of-the-art approaches.

II. PROPOSED APPROACH

A. Overview

The block diagram of the proposed approach is presented in Fig. 1. It consists of two steps: LBP-structure optimization and LBP feature generation. After deriving the optimal LBP structures, they are used to generate LBP features. Compared with previous data-driven LBP structures [10], we have added two structural regularization constraints: symmetry constraint and uniformity constraint.

The most popular LBP structure used for scene classification consists of eight nearest neighbors [7], [9] highlighted in yellow in Fig. 2. Such a structure could not capture the image characteristics at a larger scale. If we extend it to a larger 5×5 neighborhood shown in Fig. 2, the feature dimension dramatically increases to $2^{24} = 16\,777\,216$, which is too high to handle.

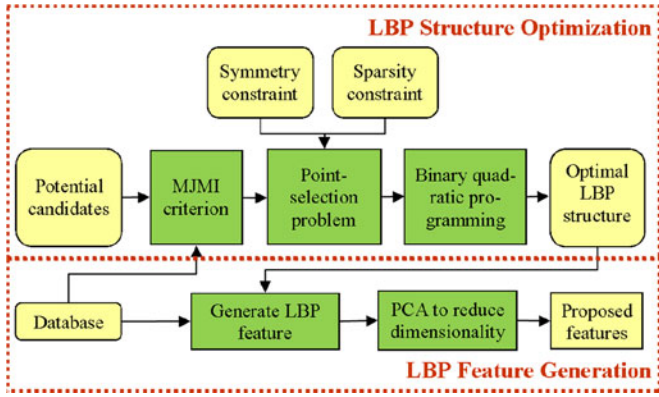


Fig. 1. Block diagram of the proposed approach to extract LBP features.

X_9	X_{10}	X_{11}	X_{12}	X_{13}
X_{24}	X_1	X_2	X_3	X_{14}
X_{23}	X_8	I_c	X_4	X_{15}
X_{22}	X_7	X_6	X_5	X_{16}
X_{21}	X_{20}	X_{19}	X_{18}	X_{17}

Fig. 2. Potential candidates for scene classification.

We thus treat the binarized-pixel-difference features shown in Fig. 2 as potential candidates, and select a predefined number of points from them to form an optimal LBP structure that could well capture the image characteristics of the target application.

Formally, denote $z_i = C_i - I_c$ as the pixel difference between the neighboring pixel C_i and the center pixel I_c . The binarized pixel difference is defined as

$$x_i = \begin{cases} 1 & \text{if } z_i \geq 0, \\ 0 & \text{if } z_i < 0. \end{cases} \quad (1)$$

Point C_i is now represented by its binarized pixel difference x_i . We cast the LBP-structure optimization as a point-selection problem: given a set of potential candidates $\mathbf{x} = \{x_i, i = 1, 2, \dots, n\}$ and target classification variable c , the goal is to find a subset of m candidates $\mathbf{x}_m \subseteq \mathbf{x}$ that optimally characterizes c .

B. LBP Structure Optimization by Using MJMI Criterion

For feature selection, it is desirable to maximize the dependency of selected features on classification variable c (Max-Dependency) [38]. We use mutual information to characterize the dependency. The goal is to find $\mathbf{x}_m \subseteq \mathbf{x}$ so that

$$\mathbf{x}_m^* = \operatorname{argmax}_{\mathbf{x}_m} I(\mathbf{x}_m; c) \quad (2)$$

$$I(\mathbf{x}_m; c) = \int \int p(\mathbf{x}_m, c) \log \frac{p(\mathbf{x}_m, c)}{p(\mathbf{x}_m)p(c)} d\mathbf{x}_m dc. \quad (3)$$

It is difficult to reliably estimate $p(\mathbf{x}_m)$ and $p(\mathbf{x}_m, c)$ due to the limited number of samples available and the large number of joint states to be estimated. In [10], a maximal-conditional-mutual-information (MJMI) criterion was utilized for LBP structure optimization. Instead of maximizing intractable $I(\mathbf{x}_m; c)$, the goal is to find a subset $\mathbf{x}_m \subseteq \mathbf{x}$ that

maximizes its approximation $\sum_{i \neq j} I(x_i, x_j; c)$, i.e.

$$\mathbf{x}_m^* = \operatorname{argmax}_{\mathbf{x}_m} \sum_{x_i, x_j \in \mathbf{x}_m, i \neq j} I(x_i, x_j; c). \quad (4)$$

To derive a globally optimal solution, (4) is converted into a binary quadratic programming problem. Denote $\mathbf{a} = (a_1, a_2, \dots, a_n)^T$, $a_i \in \{0, 1\}$ as the indication vector for \mathbf{x} , i.e., $a_i = 1$ means x_i is selected and $a_i = 0$ otherwise. Equation (4) is equivalent to

$$\mathbf{a}^* = \operatorname{argmax}_{\mathbf{a}} \mathbf{a}^T \mathbf{M} \mathbf{a}, \text{ s.t. } \sum_{i=1}^n a_i = m \quad (5)$$

where $\mathbf{M} \in \mathcal{R}^{n \times n}$, and its diagonal elements are zero and off-diagonal elements $M_{i,j} = I(x_i, x_j; c)$.

The joint probability mass function $p(x_i, x_j, c)$ can be estimated efficiently. Denote $h_{p,q}$ as the joint histogram for features x_i, x_j using q th sample of p th class. $p(x_i, x_j | c)$ is estimated as

$$p(x_i, x_j | c = p) \leftarrow \frac{1}{N_p} \sum_q h_{p,q} \quad (6)$$

where N_p is the number of samples for class p . Then, $p(x_i, x_j, c = p) = p(x_i, x_j | c = p)p(c = p)$, where $p(c = p) = N_p/N$ and N is the total number of samples.

C. Structural Constraints

The optimal LBP structure derived by (5) may overfit the training samples due to the limited number of training samples. To solve this problem, we propose two regularization constraints: symmetry constraint and uniformity constraint.

1) *Symmetry Constraint*: Most handcrafted LBP structures are symmetric about the horizontal axis, the vertical axis and the center pixel. We thus enforce the data-driven LBP structures to be symmetric. Formally, we define the x -axis (the horizontal axis) symmetry matrix $\mathbf{P}_x \in \mathcal{R}^{n \times n}$ as

$$\mathbf{P}_x(i, j) = \begin{cases} 1 & \text{if } x_i \text{ and } x_j \text{ are } x\text{-axis symmetric,} \\ 0 & \text{otherwise.} \end{cases} \quad (7)$$

Take the candidates in Fig. 2 as an example. x_3 and x_5 are x -axis symmetric. Thus, $\mathbf{P}_x(3, 5) = 1$. Clearly, $\mathbf{P}_x^T = \mathbf{P}_x$.

The indicate vector \mathbf{a}_x that is x -axis symmetric to \mathbf{a} can be obtained by $\mathbf{a}_x = \mathbf{P}_x \mathbf{a}$. We then define the x -axis symmetry measure as

$$\begin{aligned} S_x &= -(\mathbf{a}_x - \mathbf{a})^T (\mathbf{a}_x - \mathbf{a}) \\ &= -\mathbf{a}^T \tilde{\mathbf{P}}_x \mathbf{a} \end{aligned} \quad (8)$$

where $\tilde{\mathbf{P}}_x = (\mathbf{P}_x - \mathbf{I})^T (\mathbf{P}_x - \mathbf{I})$, and \mathbf{I} is the identity matrix. If \mathbf{a} is symmetric about the x -axis, \mathbf{a}_x will be the same as \mathbf{a} , and hence $S_x = 0$. Otherwise, S_x will be a negative value. A larger S_x indicates a higher symmetry about the x -axis.

Similarly, we define the symmetry measure S_y about the y -axis and S_c about the center pixel as follow:

$$S_y = -\mathbf{a}^T \tilde{\mathbf{P}}_y \mathbf{a}, \quad (9)$$

$$S_c = -\mathbf{a}^T \tilde{\mathbf{P}}_c \mathbf{a} \quad (10)$$

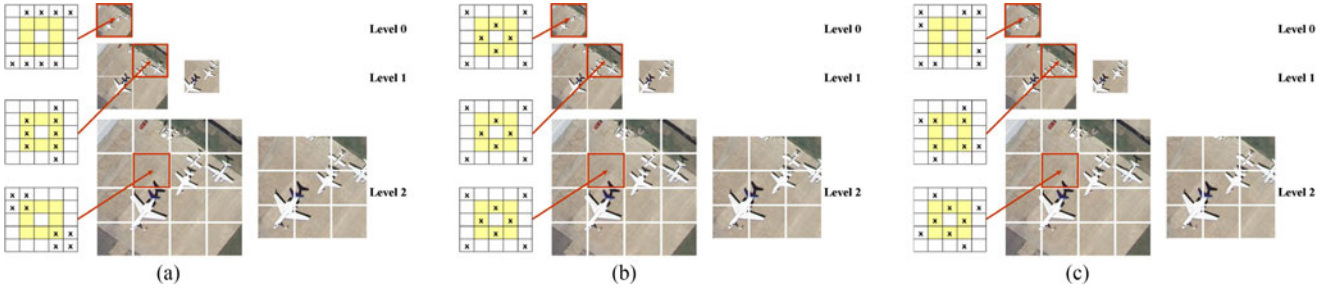


Fig. 3. Optimal LBP structures for the 21-land-use dataset without using structural constraints, using structural constraints only, and using the proposed approach are shown in (a) Without using structural constraints, (b) Using structural constraints only, and (c) Using the proposed approach respectively.

where $\tilde{\mathbf{P}}_y$ and $\tilde{\mathbf{P}}_c$ are similarly defined as $\tilde{\mathbf{P}}_x$. The final symmetry measure is:

$$S = S_x + S_y + S_c = -\mathbf{a}^T \tilde{\mathbf{P}} \mathbf{a} \quad (11)$$

where $\tilde{\mathbf{P}} = \tilde{\mathbf{P}}_x + \tilde{\mathbf{P}}_y + \tilde{\mathbf{P}}_c$. Our target is to maximize the symmetry measure S , i.e.

$$\mathbf{a}^* = \underset{\mathbf{a}}{\operatorname{argmax}} -\mathbf{a}^T \tilde{\mathbf{P}} \mathbf{a}, \text{ s.t. } \sum_{i=1}^n a_i = m. \quad (12)$$

2) *Uniformity Constraint*: The goal of the uniformity constraint is to uniformly distribute the selected points, in order to avoid the scenario that many selected points are closely clustered. Denote $\mathbf{D} \in \mathcal{R}^{n \times n}$ as the distance matrix, and its entry $D_{ij} = D(x_i, x_j)$ is the Euclidean distance between point x_i and point x_j . For example, $D(x_3, x_{14}) = 1$ for the candidates shown in Fig. 2. We achieve the uniformity by maximizing the following objective function:

$$\mathbf{x}^* = \underset{\mathbf{x}}{\operatorname{argmax}} \sum_{i=1}^m \min_{x_j} D(x_i, x_j), x_i, x_j \in \mathbf{x}_m. \quad (13)$$

This criterion maximizes the sum of the distances of all selected candidates to their nearest candidates, which ensures all selected candidates are well separated. However, deriving a globally optimal solution to (13) is NP-hard. We thus propose an alternative objective function:

$$\mathbf{x}^* = \underset{\mathbf{x}}{\operatorname{argmax}} \sum_{x_i, x_j} D(x_i, x_j), x_i, x_j \in \mathbf{x}_m. \quad (14)$$

This objective function maximizes the sum of the distances of all pairs of selected candidates. Equation (14) can be rewritten into matrix form

$$\mathbf{a}^* = \underset{\mathbf{a}}{\operatorname{argmax}} \mathbf{a}^T \mathbf{D} \mathbf{a}, \text{ s.t. } \sum_{i=1}^n a_i = m. \quad (15)$$

Equation (15) can be solved as a binary-quadratic-programming problem. Approximately, it uniformly distributes the selected candidates in the neighborhood. However, the selected candidates tend to be all boundary neighbors under this criterion. It may not select the inner candidates. As such, the derived LBP structure is not as uniform as we expect by using (13).

Therefore, we propose a new definition of the distance matrix \mathbf{D} in (15). By enforcing the symmetry constraint, we expect the derived LBP structures to be symmetric. We thus define \mathbf{D} as

$$D_{ij} = \min_{y_j \in \Theta(x_j)} D(x_i, y_j) \quad (16)$$

TABLE I
COMPARISONS WITH THE STATE OF THE ART IN TERMS OF RECOGNITION RATE ON 21-LAND-USE AND 8-EVENT DATASETS

Method	21-land-use	8-event
AdaBoost bin selection [33]	82.7%	80.2%
LQP $Disc_3^*$ [35]	83.0%	78.9%
CENTRIST [7]	85.9%	78.3%
DFD [18]	62.8%	75.7%
Discriminative LBP [14]	73.4%	66.5%
SPCK [36]	73.1%	–
SPCK+ [36]	76.1%	–
SPCK++ [36]	77.3%	–
Scene/Object model + SIFT [37]	–	73.4%
BRSP [41]	77.8%	79.6%
MJMI [10]	87.2%	84.0%
Proposed MJMI + Symmetry	88.1%	84.5%
Proposed MJMI + Uniformity	87.6%	84.7%
Proposed MJMI + Symmetry + Uniformity	88.5%	85.5%

where $\Theta(x_j)$ is the group of candidates that are x -axis, y -axis, or center symmetric to x_j . $\Theta(x_j)$ includes x_j itself. The distance matrix \mathbf{D} can be precomputed. By using the symmetry constraint (12) and the uniformity constraint [(15) with the distance matrix (16)], we could derive the LBP structures shown in Fig. 3(b).

D. LBP Structure Optimization With Structural Constraints

Equations (5), (12), and (15) are three objective functions that could be solved via binary quadratic programming. We thus combine them as one objective function:

$$\mathbf{a}^* = \underset{\mathbf{a}}{\operatorname{argmax}} \mathbf{a}^T (\mathbf{M} - \lambda_1 \tilde{\mathbf{P}} + \lambda_2 \mathbf{D}) \mathbf{a}, \text{ s.t. } \sum_{i=1}^n a_i = m \quad (17)$$

where λ_1 and λ_2 are weighting factors. \mathbf{M} , \mathbf{D} , and $\tilde{\mathbf{P}}$ are normalized by dividing by its maximum value. For simplicity, we set $\lambda_1 = \lambda_2 = \lambda$, i.e., two regularization constraints are equally important. As most entries of $\tilde{\mathbf{P}}$ are zeros, we expect $\lambda \gg 1$. In the experiments, we set $\lambda = 100$. The objective function (17) is a binary-quadratic-programming problem, which can be efficiently solved by the branch-and-bound algorithm [39]. More details can be found in [10].

III. EXPERIMENTAL RESULTS

We conduct the experiments on the 21-land dataset [36] and the eight-event dataset [37]. We compare the proposed approach with predefined LBP structures, unconstrained data-driven LBP structures, and other state-of-the-art approaches.

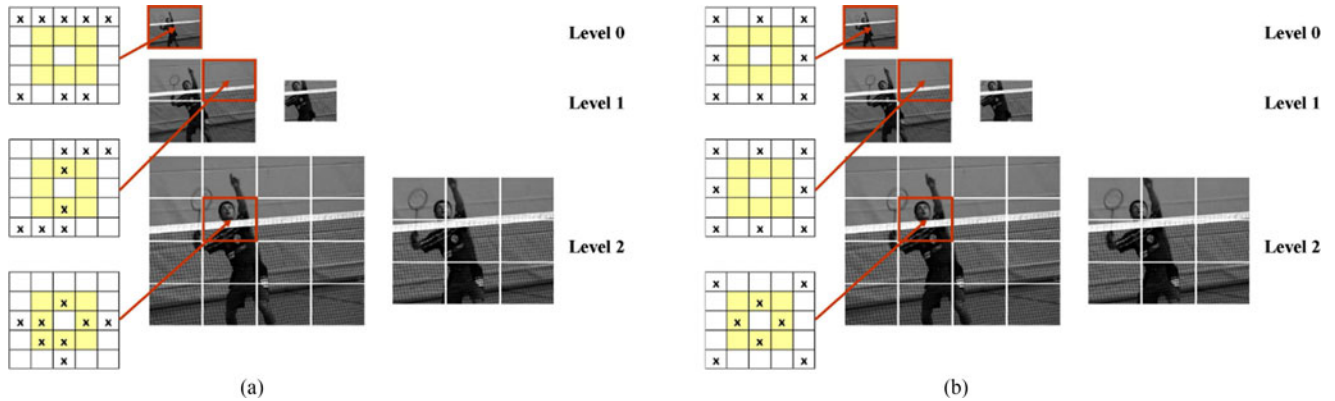


Fig. 4. Optimal LBP structures for the eight-event dataset without and with using structural constraints are shown in (a) and (b), respectively. (a) Without using structural constraints, and (b) Using the proposed approach respectively.

A. Scene Recognition on the 21-Land-Use Dataset

The 21-land-use dataset [36] contains 21 classes of aerial orthoimagery. Each class has 100 images of 256×256 pixels. We utilize the spatial pyramid [40]. The image is hierarchically divided into 31 patches as shown in Fig. 3. One optimal LBP structure is derived for each patch. We follow the same setup as in [7], [10], [36], and [41]. For each class, the images are randomly split into five equal-sized sets. Four of them are used for training and the held-out set is used for testing.

We use CENTRIST [7] as the baseline algorithm, which utilizes eight nearest neighbors as the LBP structure. We also construct the optimal LBP structures using eight points. Some examples of the optimal LBP structures derived without using structural constraints, by using structural constraints only and by the proposed approach are shown in Fig. 3(a)–(c), respectively. Without using structural constraints, the optimal structures are not symmetric, or clustered in some directions, as shown in Fig. 3(a). The optimal structures in Fig. 3(b) are solely determined by structural constraints, and hence they are the same for all patches. The optimal LBP structures derived by the proposed approach in Fig. 3(c) are different for different patches, which better capture the intrinsic image characteristics of different image patches.

We compare the proposed approach with:

- 1) Direct feature selection/extraction from the LBP-histogram bins: Adaboost bin selection [33], k-means bin clustering by LQP [35], and PCA dimension reduction by CENTRIST [7].
- 2) Other LBP-structure-learning approaches: discriminant face descriptor (DFD) [18] and discriminative LBP structure learning using a heuristic hill-climbing technique [14].
- 3) Other state-of-the-art solutions for scene recognition: SPCK, SPCK+, SPCK++ [36], and BRSP [41].
- 4) The optimal LBP structures derived by MJMI [10] without using structural constraints, and using symmetry constraint or uniformity constraint only.

The comparison results are shown in Table I. CENTRIST utilizes eight nearest neighbors highlighted in yellow. It achieves fairly good performance. MJMI [10] optimizes the LBP structures in a data-driven way, and significantly outperforms other compared approaches. By incorporating structural constraints into the LBP-structure optimization, the proposed approach significantly outperforms MJMI and all other approaches.

Compared to MJMI [10] without using structural constraints, the proposed approach improves the recognition rate from 87.2% to 88.5%, which demonstrates the effectiveness of the proposed approach.

B. Scene Recognition on the Eight-Event Dataset

The eight-event dataset [37] is composed of eight sport classes. Each class has 137 to 250 high-resolution images. To capture the image micro-structures at the same scale, we resize the image so that its minimum dimension (height or weight) is 600. The experiments are repeated five times. For each trial, we randomly select 70 images per class for training and 60 for testing, same as in [7], [10], [37], and [41]. Other setups are the same as for the 21-land-use dataset. Some examples of the optimal LBP structures derived without using structural constraints and by using the proposed approaches are shown in Fig. 4(a) and (b), respectively. The structural constraints regularize the LBP structures to be symmetric and scattered.

From the results shown in Table I, we can see that CENTRIST does not perform well on the eight-event dataset. By optimizing LBP structures, MJMI significantly outperforms other compared approaches, including structure-learning approaches, such as DFD [18] and discriminative LBP [14]. The proposed approach further boosts the performance by regularizing the LBP structures using the structural constraints. It increases the recognition rate of MJMI by 1.5%.

IV. CONCLUSION

Handcrafted LBP structures are designed using human knowledge on images. They are simple and easy to use, but they cannot optimally capture the intrinsic image characteristics of the target application. On the other hand, previous data-driven LBP structures are fine-tuned for the target application, but they may overfit the training samples. To address these problems, we propose a way to incorporate the human knowledge into the LBP-structure optimization. We derive two structural regularization constraints, symmetry constraint and uniformity constraint, from handcrafted LBP structures. Those two constraints are designed in such a way that they can be solved efficiently by binary quadratic programming. The proposed approach is evaluated on two scene-classification datasets. It demonstrates superior performance compared with other state-of-the-art approaches.

REFERENCES

- [1] Z. Li, G. Liu, Y. Yang, and J. You, "Scale-and rotation-invariant local binary pattern using scale-adaptive texton and subuniform-based circular shift," *IEEE Trans. Image Process.*, vol. 21, no. 4, pp. 2130–2140, Apr. 2012.
- [2] K. Wang, C.-E. Bichot, C. Zhu, and B. Li, "Pixel to patch sampling structure and local neighboring intensity relationship patterns for texture classification," *IEEE Signal Process. Lett.*, vol. 20, no. 9, pp. 853–856, Sep. 2013.
- [3] T. Song *et al.*, "Noise-robust texture description using local contrast patterns via global measures," *IEEE Signal Process. Lett.*, vol. 21, no. 1, pp. 93–96, Jan. 2014.
- [4] G. Zhao and M. Pietikainen, "Dynamic texture recognition using local binary patterns with an application to facial expressions," *IEEE Trans. Pattern Anal. Mach. Intell.*, vol. 29, no. 6, pp. 915–928, Jun. 2007.
- [5] G. Zhao, T. Ahonen, J. Matas, and M. Pietikainen, "Rotation-invariant image and video description with local binary pattern features," *IEEE Trans. Image Process.*, vol. 21, no. 4, pp. 1465–1477, Apr. 2012.
- [6] J. Ren, X. Jiang, and J. Yuan, "Dynamic texture recognition using enhanced LBP features," in *Proc. Int. Conf. Acoust., Speech, Signal Process.*, 2013, pp. 2400–2404.
- [7] J. Wu and J. Rehg, "CENTRIST: A visual descriptor for scene categorization," *IEEE Trans. Pattern Anal. Mach. Intell.*, vol. 33, no. 8, pp. 1489–1501, Aug. 2011.
- [8] J. Ren, X. Jiang, and J. Yuan, "Learning binarized pixel-difference pattern for scene recognition," in *Proc. Int. Conf. Image Process.*, 2013, pp. 2494–2498.
- [9] Y. Xiao, J. Wu, and J. Yuan, "mCENTRIST: A multi-channel feature generation mechanism for scene categorization," *IEEE Trans. Image Process.*, vol. 23, no. 2, pp. 823–836, Feb. 2014.
- [10] J. Ren, X. Jiang, J. Yuan, and G. Wang, "Optimizing LBP structure for visual recognition using binary quadratic programming," *IEEE Signal Process. Lett.*, vol. 21, no. 11, pp. 1346–1350, Nov. 2014.
- [11] T. Ahonen, A. Hadid, and M. Pietikainen, "Face description with local binary patterns: Application to face recognition," *IEEE Trans. Pattern Anal. Mach. Intell.*, vol. 28, no. 12, pp. 2037–2041, Dec. 2006.
- [12] W. Zhang, S. Shan, X. Chen, and W. Gao, "Local gabor binary patterns based on Kullback-Leibler divergence for partially occluded face recognition," *IEEE Signal Process. Lett.*, vol. 14, no. 11, pp. 875–878, Nov. 2007.
- [13] X. Li, W. Hu, Z. Zhang, and H. Wang, "Heat kernel based local binary pattern for face representation," *IEEE Signal Process. Lett.*, vol. 17, no. 3, pp. 308–311, Mar. 2010.
- [14] D. Maturana, D. Mery, and A. Soto, "Learning discriminative local binary patterns for face recognition," in *Proc. IEEE Int. Conf. Face Gesture Recognit. Workshops*, 2011, pp. 470–475.
- [15] J. Ren, X. Jiang, and J. Yuan, "Relaxed local ternary pattern for face recognition," in *Proc. Int. Conf. Image Process.*, 2013, pp. 3680–3684.
- [16] X. Huang, G. Zhao, W. Zheng, and M. Pietikainen, "Spatiotemporal local monogenic binary patterns for facial expression recognition," *IEEE Signal Process. Lett.*, vol. 19, no. 5, pp. 243–246, May 2012.
- [17] J. Ren, X. Jiang, and J. Yuan, "Noise-resistant local binary pattern with an embedded error-correction mechanism," *IEEE Trans. Image Process.*, vol. 22, no. 10, pp. 4049–4060, Oct. 2013.
- [18] L. Zhen, M. Pietikainen, and S. Li, "Learning discriminant face descriptor," *IEEE Trans. Pattern Anal. Mach. Intell.*, vol. 36, no. 2, pp. 289–302, Feb. 2014.
- [19] J. Ren, X. Jiang, and J. Yuan, "Quantized fuzzy LBP for face recognition," in *Proc. Int. Conf. Acoust., Speech, Signal Process.*, 2015, pp. 1503–1507.
- [20] X. Wang, T. Han, and S. Yan, "An HOG-LBP human detector with partial occlusion handling," in *Proc. IEEE Int. Conf. Comput. Vis.*, 2009, pp. 32–39.
- [21] J. Xu, Q. Wu, J. Zhang, and Z. Tang, "Fast and accurate human detection using a cascade of boosted MS-LBP features," *IEEE Signal Process. Lett.*, vol. 19, no. 10, pp. 676–679, Oct. 2012.
- [22] A. Satpathy, X. Jiang, and H. Eng, "LBP based edge-texture features for object recognition," *IEEE Trans. Image Process.*, vol. 23, no. 5, pp. 1953–1964, May 2014.
- [23] J. Ren, X. Jiang, and J. Yuan, "Learning LBP structure by maximizing the conditional mutual information," *Pattern Recognit.*, vol. 48, no. 10, pp. 3180–3190, 2015.
- [24] L. Nanni and A. Lumini, "Local binary patterns for a hybrid fingerprint matcher," *Pattern Recognit.*, vol. 41, no. 11, pp. 3461–3466, 2008.
- [25] J. Ren, X. Jiang, and J. Yuan, "A chi-squared-transformed subspace of LBP histogram for visual recognition," *IEEE Trans. Image Process.*, vol. 24, no. 6, pp. 1893–1904, Jun. 2015.
- [26] M. Heikkilä, M. Pietikäinen, and C. Schmid, "Description of interest regions with local binary patterns," *Pattern Recognit.*, vol. 42, no. 3, pp. 425–436, 2009.
- [27] J. Ren, X. Jiang, and J. Yuan, "LBP encoding schemes jointly utilizing the information of current bit and other LBP bits," *IEEE Signal Process. Lett.*, vol. 22, no. 12, pp. 2373–2377, Dec. 2015.
- [28] C. Heng, S. Yokomitsu, Y. Matsumoto, and H. Tamura, "Shrink boost for selecting multi-LBP histogram features in object detection," in *Proc. IEEE Conf. Comput. Vis. Pattern Recognit.*, 2012, pp. 3250–3257.
- [29] J. Ren, X. Jiang, and J. Yuan, "Sound-event classification using pseudo-color CENTRIST feature and classifier selection," in *Proc. Int. Workshop Pattern Recognit.*, 2016, pp. 100111C-1–100111C-5, doi: 10.1117/12.2242357.
- [30] J. Ren, X. Jiang, J. Yuan, and N. Magnenat-Thalmann, "Sound-event classification using robust texture features for robot hearing," *IEEE Trans. Multimedia*, vol. PP, no. 99, p. 1, 2016, doi: 10.1109/TMM.2016.2618218.
- [31] Y. Mu, S. Yan, Y. Liu, T. Huang, and B. Zhou, "Discriminative local binary patterns for human detection in personal album," in *Proc. IEEE Conf. Comput. Vision Pattern Recognit.*, 2008, pp. 1–8.
- [32] C. Shan and T. Gritti, "Learning discriminative LBP-histogram bins for facial expression recognition," in *Proc. Brit. Mach. Vis. Conf.*, 2008, pp. 1–10.
- [33] C. Shan, "Learning local binary patterns for gender classification on real-world face images," *Pattern Recognit. Lett.*, vol. 33, no. 4, pp. 431–437, 2012.
- [34] Z. Cao, Q. Yin, X. Tang, and J. Sun, "Face recognition with learning-based descriptor," in *Proc. IEEE Conf. Comput. Vis. Pattern Recog.*, 2010, pp. 2707–2714.
- [35] S. ul Hussian and B. Triggs, "Visual recognition using local quantized patterns," in *Proc. Eur. Conf. Comput. Vis.*, 2012, pp. 716–729.
- [36] Y. Yang and S. Newsam, "Spatial pyramid co-occurrence for image classification," in *Proc. IEEE Int. Conf. Comput. Vis.*, 2011, pp. 1465–1472.
- [37] L. Li and L. Fei-Fei, "What, where and who? classifying events by scene and object recognition," in *Proc. IEEE Int. Conf. Comput. Vis.*, 2007, pp. 1–8.
- [38] H. Peng, F. Long, and C. Ding, "Feature selection based on mutual information criteria of max-dependency, max-relevance, and min-redundancy," *IEEE Trans. Pattern Anal. Mach. Intell.*, vol. 27, no. 8, pp. 1226–1238, Aug. 2005.
- [39] R. Horst, P. M. Pardalos, and H. E. Romeijn, *Handbook of Global Optimization*, New York, NY, USA: Springer, 2002.
- [40] S. Lazebnik, C. Schmid, and J. Ponce, "Beyond bags of features: Spatial pyramid matching for recognizing natural scene categories," in *Proc. IEEE Conf. Comput. Vis. Pattern Recognit.*, 2006, pp. 2169–2178.
- [41] Y. Jiang, J. Yuan, and G. Yu, "Randomized spatial partition for scene recognition," in *Proc. Eur. Conf. Comput. Vis.*, 2012, pp. 730–743.